

## Characterization and comparison of titanium dioxide nanoparticles prepared by microwave and pulse laser ablation liquid methods

Mariam Khaled Glob<sup>1</sup> Saleem Azara Hussain<sup>2</sup> Khalidah H. Al-Mayalee<sup>1</sup>

<sup>1</sup> Department of Physics, College of Education for Girls, University of Kufa, AL-Najaf, Iraq.

<sup>2</sup> Department of Physics, College of Education, University of Al-Qadisiyah, AL-Diwaniyah, Iraq

Corresponding author: [mmkk909084@gmail.com](mailto:mmkk909084@gmail.com)

### ARTICLE INF.

#### Article history:

Received: 26 NOV., 2023

Revised: 11 JAN., 2024

Accepted: 7 FEB., 2024

Available Online: 24 JUN., 2024

#### Keywords:

Nanoparticles,  
Titanium Isopropoxide  
Laser ablation  
Nd:YAG laser,  
titanium dioxide

### ABSTRACT

In this study titanium dioxide ( $\text{TiO}_2$ ) was synthesized quickly and cheaply using microwaves and pulsed laser ablation. Titanium isopropoxide ( $\text{Ti}[\text{OCH}(\text{CH}_3)_2]_4$ ) was the precursor and deionized water (DIW) was the solvent and reducer for sub-micrometer particle production in microwave technique.  $\text{TiO}_2$  nanoparticles were synthesized in pulsed laser ablation liquid medium after a 5-minute preparation period in a 1200 W commercial microwave and a 1-hour annealing at  $400^\circ\text{C}$ . A Q-switched Nd: YAG laser with 480 mJ energy per pulse was used for 100, 200, and 300 pulses. Multiple methods, including XRD, BET, and EDX. XRD showed anatase  $\text{TiO}_2$  in microwave-synthesized nanoparticles. Pulsed laser ablation produced pure  $\text{TiO}_2$  nanoparticles with a brookite crystalline structure. In microwave BET analysis,  $\text{TiO}_2$  has a large surface area of 72.727 to 108.28  $\text{m}^2/\text{g}$ . BET analysis indicated 82.44 to 98.67  $\text{m}^2/\text{g}$  of  $\text{TiO}_2$  surface area by pulsed laser ablation. Strong titanium (Ti) and oxygen (O) peaks in microwave and pulsed laser ablation EDX tests showed nanoparticle purity.

DOI: <https://doi.org/10.31257/2018/JKP/2024/v16.i01.14196>

## توصيف ومقارنة جزيئات ثاني أكسيد التيتانيوم النانوية المحضرة بواسطة الميكروويف وطريقة الاستئصال بالليزر النبضي

خالدة حبيب<sup>1</sup>

سليم عزارة حسين<sup>2</sup>

مريم خالد جلوب<sup>1</sup>

<sup>1</sup> قسم الفيزياء، كلية التربية، جامعة الكوفة، النجف، العراق

<sup>2</sup> قسم الفيزياء، كلية التربية، جامعة القادسية، الديوانية، العراق

### الكلمات المفتاحية:

الجسيمات النانوية  
إيزوبروكسيد التيتانيوم  
الاستئصال بالليزر  
ليزر Nd:YAG  
ثاني أكسيد التيتانيوم

### الخلاصة

في هذه الدراسة تم تصنيع ثاني أكسيد التيتانيوم ( $\text{TiO}_2$ ) بسرعة وبتكلفة زهيدة باستخدام الموجات الدقيقة والاستئصال بالليزر النبضي. كان إيزوبروكسيد التيتانيوم ( $\text{Ti}[\text{OCH}(\text{CH}_3)_2]_4$ ) هو المادة الأولية وكان الماء منزوع الأيونات (DIW) هو المذيب والمخفض لإنتاج الجسيمات دون الميكرو مترية في تقنية الميكروويف. تم تصنيع الجسيمات النانوية  $\text{TiO}_2$  في وسط سائل للاستئصال بالليزر النبضي بعد فترة تحضير مدتها 5 دقائق في ميكروويف تجاري بقدرة 1200 واط وتليدين لمدة ساعة عند  $400^\circ\text{C}$  درجة مئوية. تم استخدام ليزر Q-switched Nd:YAG بطاقة 480 مللي جول لـ 100 و 200 و 300 نبضة. تم استخدام طرق متعددة لفحص

العينات، بما في ذلك XRD، BET، وEDX. أظهر نتائج XRD ان المادة المحضرة بطريقة المايكرويف كانت في طور الأاناتاز. أما نتائج XRD بطريقة الاستئصال بالليزر النبضي لجسيمات  $TiO_2$  كانت بطور البروكيت. أما نتائج تحليل BET بالموجات الدقيقة كانت العينات المحضرة ذات مساحة سطحية كبيرة تبلغ 72.727 إلى 108.28 م<sup>2</sup>/غم. أما نتائج تحليل العينات المحضرة عن طريق الاستئصال بالليزر النبضي كانت الجسيمات المحضرة ذات مساحة 82.44 إلى 98.67 م<sup>2</sup>/غم من مساحة سطح  $TiO_2$ . أظهرت نتائج EDX للعينات التي تم تحضيرها وبالطريقتين تحتوي ع قمم للتيتانيوم (Ti) والأكسجين (O) في الموجات الدقيقة والاستئصال بالليزر النبضي وهذا يدل على نقاء الجسيمات النانوية المحضرة.

## 1. INTRODUCTION

Titanium dioxide ( $TiO_2$ ), also referred to as Titania, is a white inorganic solid that is insoluble in water, thermally stable, chemically unreactive, and non-flammable. Titanium dioxide ( $TiO_2$ ) is extensively utilized in many manufacturing applications such as catalyst support, dye-sensitized photo electrochemical solar cells, and consumer products like cosmetics, coatings, paints, ceramics, printing inks, and textiles. Furthermore, the exceptional photocatalytic properties of  $TiO_2$ , including its potent oxidizing ability and non-toxic nature, have established it as a superior photocatalyst [1].

Titanium dioxide is classified as a transition metal oxide. Titanium dioxide ( $TiO_2$ ) is typically not found naturally, but rather obtained from leucoxene ores or limonite. Titanium, which ranks ninth in abundance among elements found in the earth's crust, is present as a compound in several types of rocks and mineral sands [2].

Compared to bulk material, the characteristics of  $TiO_2$  nanostructured material show a considerable influence on size. The nanostructured  $TiO_2$  has a high surface area that allows for effective adsorption and catalytic reactions.  $TiO_2$  has three prevalent

phase structures: brookite, anatase, and rutile. Various species of  $TiO_2$ , including columbite, hollandite, and ramsdellite, can be acquired.

These composites are not naturally occurring but can be synthesized in the laboratory through targeted pressure treatment of anatase and rutile phases. Out all these crystal forms, the anatase form exhibits the highest level of photoactivity. Rutile exhibits a lower electron-hole recombination rate compared to anatase, which could perhaps account for the superior photocatalytic performance of anatase over rutile.

The disparity in bandgap energy between anatase and rutile cannot be regarded as a viable explanation, given the discrepancy is insignificantly minor. Furthermore, anatase has superior performance in photocatalytic processes compared to brookite. Due to rutile's high thermodynamic stability, achieving a pure phase of anatase photocatalyst by synthesis is a difficult task [3].

The general features of these forms are presented in Table (1). Titanium dioxide ( $TiO_2$ ) exhibits excellent photo stability, affordability, chemical and biological inertness, high ambient temperature activity, safety for usage,

and is particularly well-suited for the degradation of trace-level contaminants. Figure (1) illustrates the many phases of TiO<sub>2</sub>, each having distinct phase structures that might result in variations in the chemical and physical properties of the overall material.

The aim of this study is to synthesize titanium dioxide nanoparticles using two methods. The first method is the

microwave method and the second method is pulsed laser ablation, and then the results are analyzed and interpreted. The materials obtained in this study were subjected to characterization using different analytical techniques, including X-ray diffraction (XRD), Brunauer-Emmett-Teller (BET) analysis, and field emission scanning electron microscopy (FESEM).

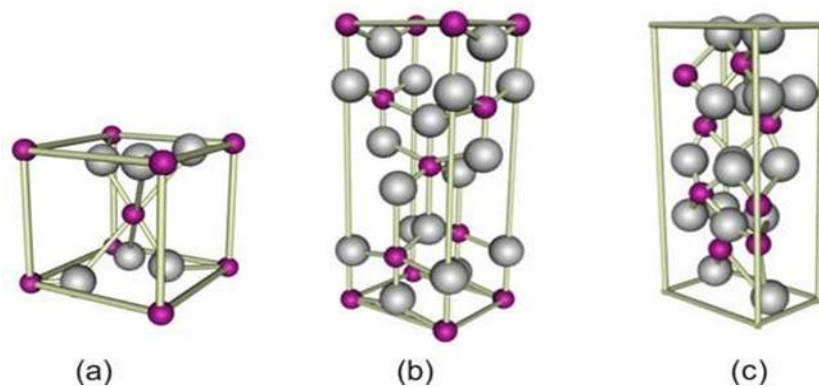


**Fig.(1):** Crystal structures of TiO<sub>2</sub> : (a) Anatase (b) Rutile (c) Brookite[4]

**Table (1):** General properties of the TiO<sub>2</sub> phases.

Crystal Structure	Anatase	Brookite	Rutile
Crystal System	Tetragonal	Rhombohedral	Tetragonal
Density (g/cm <sup>3</sup> )	3.9	4.13	4.17
Band Gap Energy (eV)	3.2	3.1-3.4	3.0
Melting Point (°C)	Transform to Rutile	Transform to Rutile	1870
Refractive Index	2.52	2.63	2.72

## 2. Experimental Part

The microwave approach was used to synthesize titanium dioxide (TiO<sub>2</sub>) powder from titanium (IV) isopropoxide (TTIP) and deionized water (DIW) as solvents and reducing agents for sub micrometer particle formation. In the synthesis, 10 ml of

TTIP was slowly added to 100 ml of DIW in a glass vessel under vigorous magnetic stirring at 600 rpm for 10 minutes. The microwave-assisted synthesis used a Sharp-38L microwave oven at 2.45 GHz for 5 minutes at 40%, 60%, and 100% of 1200W. The

solution turned milky white, indicating TiO<sub>2</sub> nanoparticle production (Figure 2-a). The precipitate was rinsed with DIW and 100% ethanol and centrifuged for 5 minutes at 4500 rpm

(Figure 2-b). After drying in an oven at 60 °C for an hour, the powder was left overnight. A furnace (ELF 11/14B) was used to calcine the powder at 400 °C in the air for 1 hour (Figure 2-c).

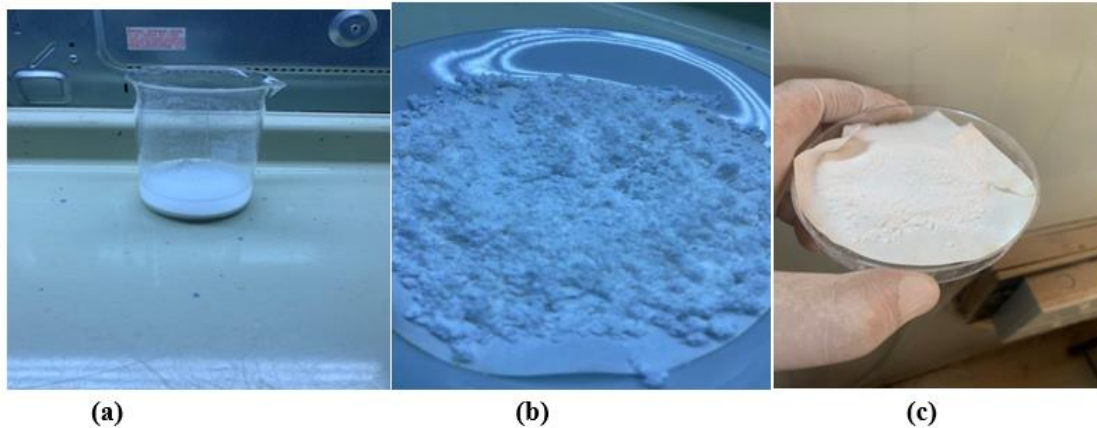


**Fig. (2):** Steps of synthesise samples: (a)The milky white solution after the titration process. (b)The collected powder after washing with ethanol and de-ionized water. (c)the final product after annealing at 400 °C for 1 h.

In Laser ablation was utilized to synthesise nanoparticles due of its simplicity and affordability. Immersing high-purity TiO<sub>2</sub> in DDDW at room temperature was the process. First, 5 grams of titanium dioxide (TiO<sub>2</sub>) was compressed in a 2-centimeter mold for 15 minutes without any extra chemicals. After placing the titanium dioxide (TiO<sub>2</sub>) at the base of a quartz container, 4 mL of liquid was added. The subjects were subjected to a 1064 nm Q-switched Nd: YAG laser. Laser pulses lasted 7nanosecondsand were repeated at 5 hertz. Laser pulses for TiO<sub>2</sub> were 480 mill joules. The crushed titanium dioxide was laser-blasted with 100, 200, and 300 pulses. Focusing the laser beam on the nanostructure causes high-energy surface interactions. The term "plasmon" was introduced then. Laser-metal surface interaction produces plasmon, electromagnetic oscillations caused by electron density variation. Plasmon impurities affect chemical reactions and enable titanium dioxide

atom diffusion. A 100-mm focusing lens focused the laser beam on the TiO<sub>2</sub> target.

### 3.Results and discussion

#### 3.1 X-ray Diffraction

Figure (3) shows the X-ray diffract grams of the synthesized TiO<sub>2</sub> nanoparticles samples. From the X-ray patterns, the peaks have affirmed the formation of nanomaterials with high crystallization. It can be deduced that the TiO<sub>2</sub> nanoparticles synthesized in this study exist in anatase TiO<sub>2</sub> phase (according to JCPDS file No.21-1272).The diffraction peaks of the prepared samples reveal a sharp domain (101) peak at about  $2\theta=25.33^\circ$  ascribed to a tetragonal structure of TiO<sub>2</sub> phase with anatase lattice constants  $a = b = 0.37852 \text{ nm}$ ,  $c = 0.65139 \text{ nm}$  and angles  $\alpha = \beta = \gamma = 90$ . The X-ray patterns also showed that there are no peaks of other materials, indicating that the samples were prepared with a high degree of the purity. The average crystalline size of TiO<sub>2</sub> nanoparticles was determined by

broadening the anatase TiO<sub>2</sub> peaks at different 2θ in the model using the Debye Scherer equation[5]. Table(2)The results showed that the average crystal size of the prepared samples 3.73nm to 8.46nm, The uniform microwave

heating mechanism resulted in homogeneous heating of the TiO<sub>2</sub> material thus obtaining this anatase phase within a very short time[6,7].

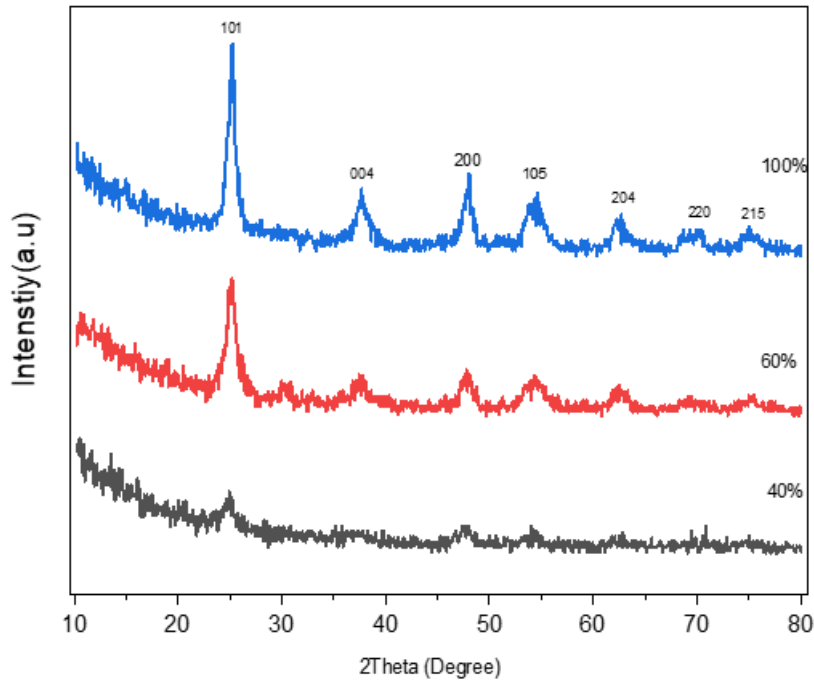


**Fig. (3):** X-ray diffract grams of the TiO<sub>2</sub> Nanoparticles.

microwave power	Average crystallite size (D) (nm)
40%	3.73
60%	5.98
100%	8.46

The results of the average crystal size showed that the samples prepared by the microwave method increased with the increase in the energy used This is consistent with the researcher's results[8].

In pulse laser ablation The X-ray diffract grams of the synthesized TiO<sub>2</sub> nanoparticle samples are illustrated in Figure4.The peaks in the X-ray patterns have confirmed the presence of nanomaterials exhibiting significant

crystallinity. The brookite TiO<sub>2</sub> phase is indicative of the TiO<sub>2</sub> nanoparticles that were synthesized in this investigation (JCPDS file No.29-1360).A distinct domain (120) peak at approximately 2θ=25.33° is observed in the diffraction patterns of the prepared samples. This peak is attributed to a Rhombohedral structure of the TiO<sub>2</sub> phase, characterized by brookite lattice constants a = b = c 0.37852 nm and angles α = β = γ ≤ 90°. Table(3) summarizes the XRD

results of TiO<sub>2</sub> nan powders prepared by the puls laser ablation, Table(2)The results showed that the average crystal

size of the prepared samples 3.30nm to 2.31nm.

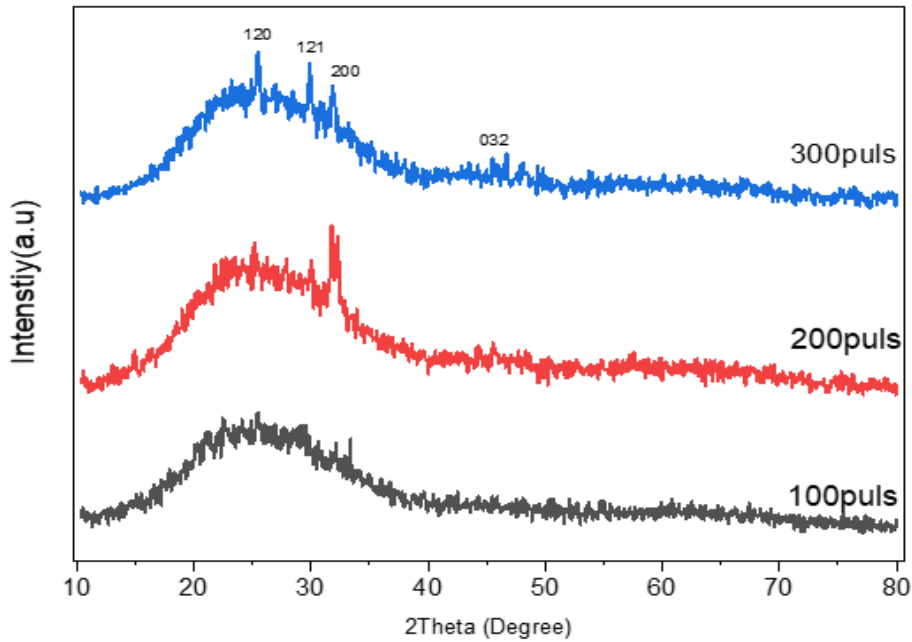


**Fig. (4):** X-ray diffract grams of the TiO<sub>2</sub> nanoparticles by laser ablation method.

**Table (3):** The average crystallite sizes of the prepared TiO<sub>2</sub> nanoparticles by laser ablation method.

Laser pulse	Average crystallite size (D) (nm)
100puls	3.30
200puls	3.03
300puls	2.31

The results of the average crystal size showed that the samples prepared by the pulse laser ablation method

**3.2 Specific Surface Area (BET)**

Figure (5,6,7) shows the results of The typical isotherm nitrogen (N<sub>2</sub>) adsorption and desorption of TiO<sub>2</sub> nanoparticles are (40%, 60%, and 100%) samples by microwave method. The relative isotherms of the samples were of Type IV, characteristics of mesoporous materials. Particles showed a relative high surface area. The specific surface areas at 40%, 60%, and 100% were 72.727 m<sup>2</sup>/g, 102.62 m<sup>2</sup>/g, and 108.28 m<sup>2</sup>/g as show in

decreases with the increase in the energy used.

Table (3). Fig.7 shows four regions. The figure shows these regions. Microspores are present in the first region, which has a relative pressure (P/P<sub>0</sub>) below 0.5 and a progressive increase in adsorption. Isotherms with weak hysteresis loops indicate mesopores in the second region, where the relative pressure is between 0.5 and 0.6[8,9]. The isotherm shows capillary concentration in the third zone for relative pressures between 0.6 and 0.92[10]. The fourth location, with the

highest relative pressure above (0.92), has a tiny hysteresis loop, indicating larger mesopores [11]. Using the Barret-Joyner-Halenda (BJH) method, the distribution pattern of the pore size was evaluated from the N<sub>2</sub> isotherm desorption branch, as shown in Fig(8,9,10).The results show that the

average pore size of the prepared samples synthesized by the microwave method (40%, 60%, 100%) is about (3.52, 3.55, and 4.02 nm)and the average pore volume is about (0.062, 0.057, 0.073, cm<sup>3</sup>g<sup>-1</sup>) as shown in Table4 This is consistent with the researcher's results[12].

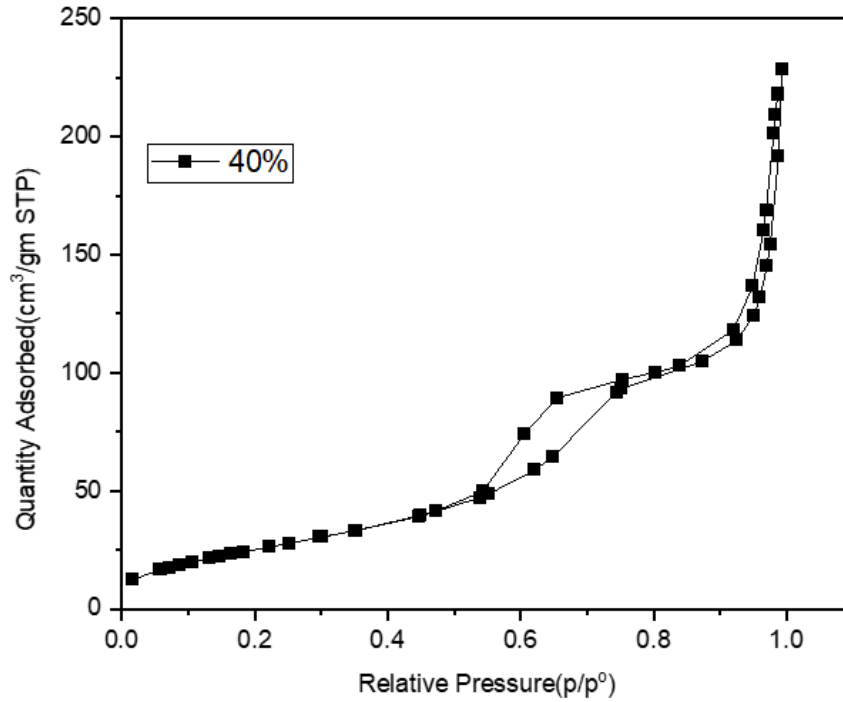


Fig. (5) (N<sub>2</sub>) adsorption-desorption of TiO<sub>2</sub> Nanoparticles at 40%.

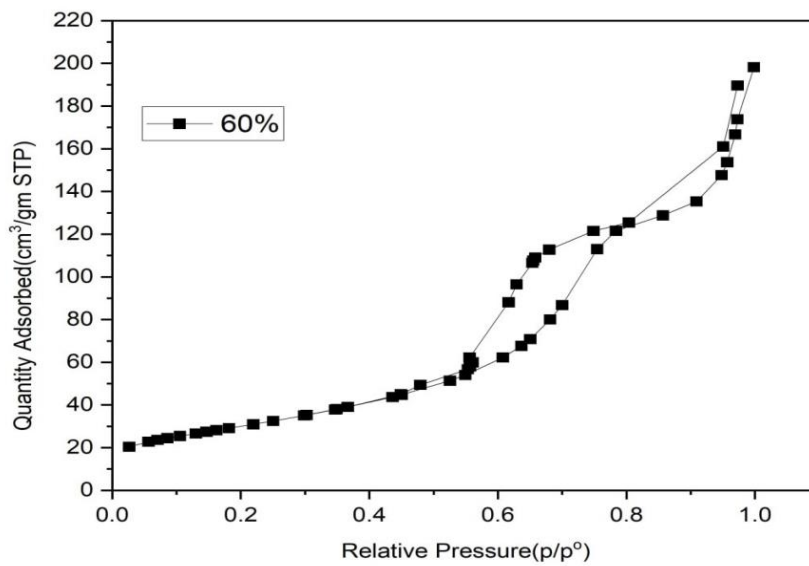


Fig. (6) (N<sub>2</sub>) adsorption-desorption of TiO<sub>2</sub> Nanoparticles at 60%.

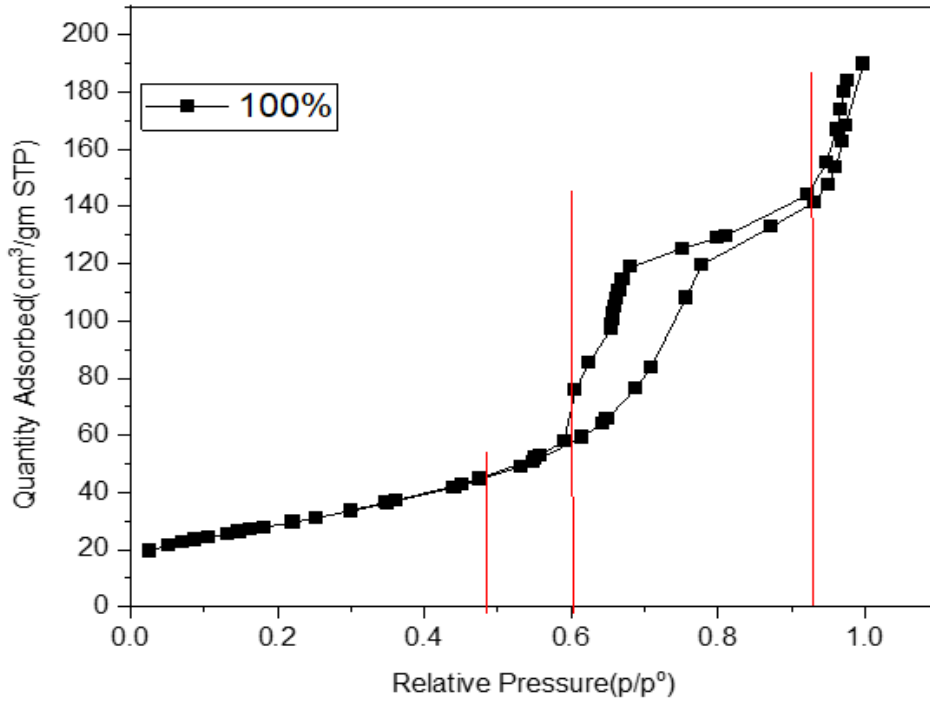


Fig. (7) (N<sub>2</sub>) adsorption-desorption of TiO<sub>2</sub> Nanoparticles at 100%.

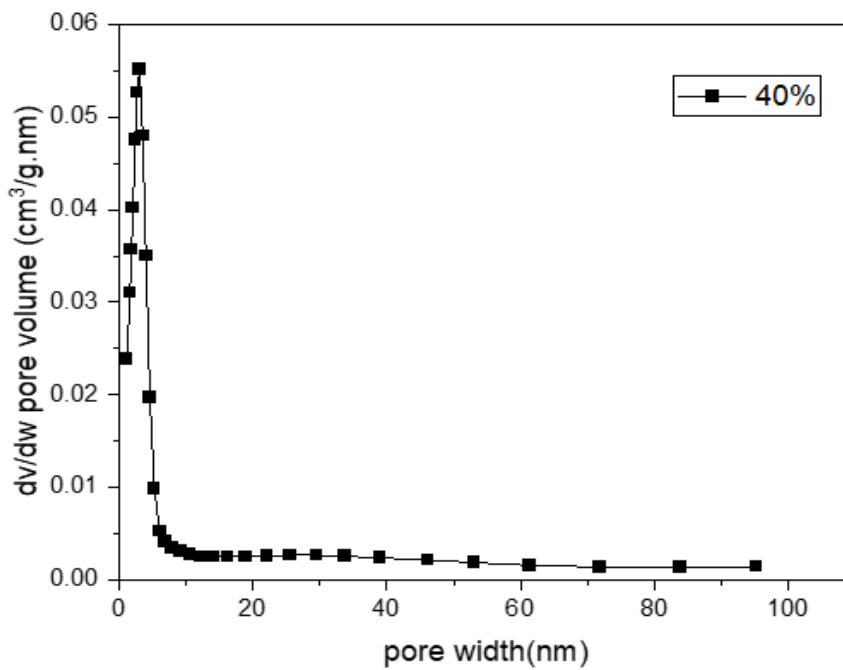


Fig. (8) Pore size distribution of TiO<sub>2</sub> Nanoparticles at 40%.



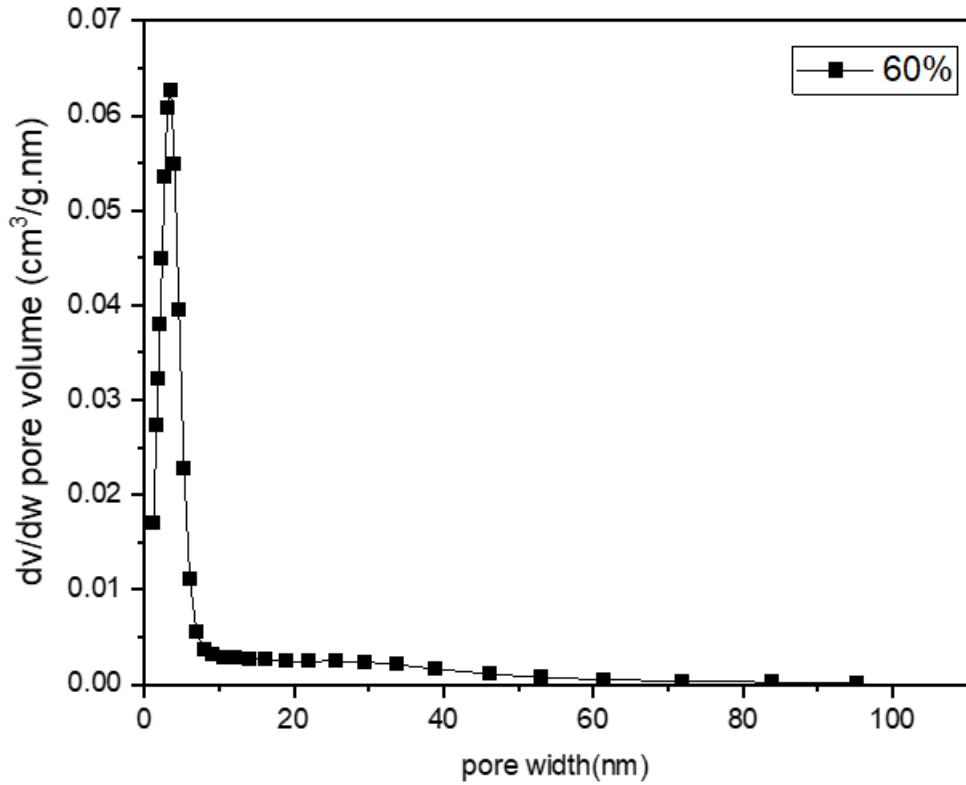


Fig. (9) Pore size distribution of TiO<sub>2</sub> Nanoparticles at 60%.

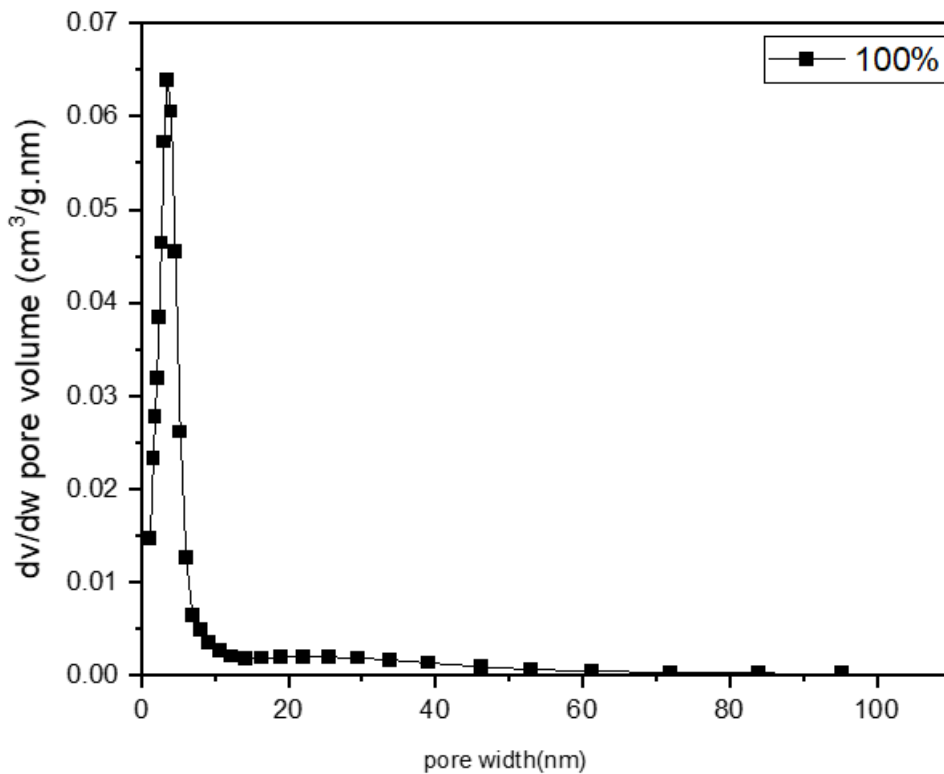


Fig. (10): Pore size distribution of TiO<sub>2</sub> Nanoparticles at 100%.

**Table (4):** Surface area, average pore diameter and volume of TiO<sub>2</sub> Nanoparticles samples prepared at (40%,60%,100%).

microwave power	Surface area (m <sup>2</sup> /g <sup>-1</sup> )	Average pore diameter (nm)	Total pore volume (m <sup>3</sup> /g)
40%	72.727	3.52	0.062
60%	102.62	4.55	0.057
100%	108.28	5.02	0.063

From Table 4, we notice that the surface area is different and the preparation can be varied at rest because the energy is sufficient and this is with the X-ray diffraction results.

Figure (11,12,13) illustrates the findings of the isotherms of nitrogen (N<sub>2</sub>) adsorption and desorption of TiO<sub>2</sub> nanoparticles by pulsed laser ablation are (100pulse, 200pulse, and 300pulse) samples. the specific surface area of TiO<sub>2</sub> nanoparticles produced by laser ablation for samples with 100puls, 200puls, and 300puls was approximately 82.44, 86.43, and 96.67 m<sup>2</sup>/ g. Figure 13 divides the area into four regions. The figure shows these regions: The isotherm shows a progressive rise in adsorption in the first region, where P/P<sub>0</sub> is smaller than 0.37, indicating microspores. Mesopores are suggested by faint hysteresis loops on the isotherm in the second region, where the relative

pressure ranges from 0.37 to 0.46. The isotherm has capillaries in the third zone, with relative pressures from 0.45 to 0.96. This shows that the hysterical loop in this location is broad and distinct compared to others. This suggests different capillary concentrations. Additionally, it shows the association between ambient phase adsorbate and adsorbent surface adsorbate under constant temperature and equilibrium conditions. The fourth region has the highest relative pressure (0.96).

Using the Barret-Joyner-Halenda (BJH) method, the distribution pattern of the pore size was evaluated from the N<sub>2</sub> isotherm desorption branch, as shown in Fig (14,15,16). The results show that the average pore size of the prepared samples synthesized by the microwave method (100 pulse, 200 pulse, 300 pulse) is about (3.52, 3.57, and 5.28 nm) as Table5.

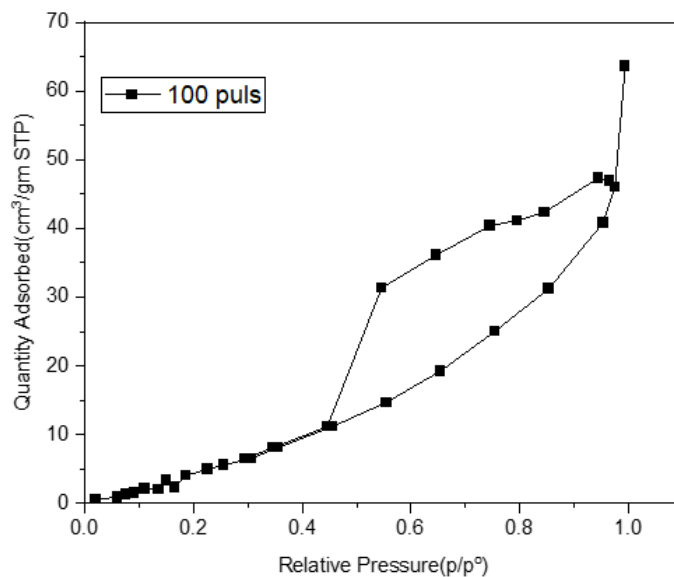


Fig.(11) (N<sub>2</sub>)adsorption-desorption of TiO<sub>2</sub> nanoparticles at 100puls.

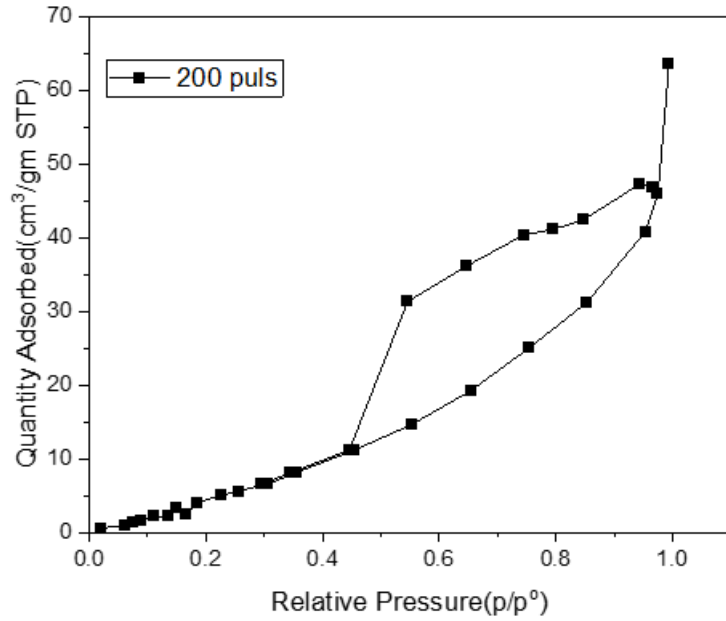


Fig. (12) (N<sub>2</sub>) adsorption-desorption of TiO<sub>2</sub> nanoparticles at 200puls.

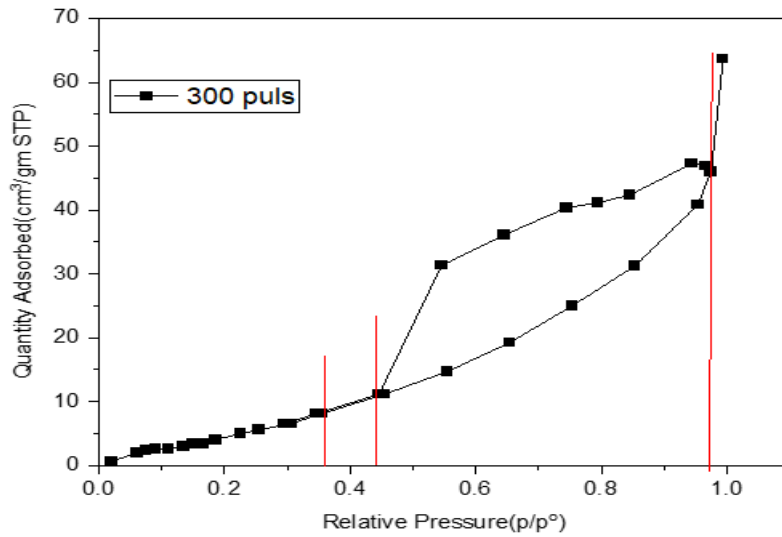


Fig. (13) (N<sub>2</sub>) adsorption-desorption of TiO<sub>2</sub> nanoparticles at 300puls.

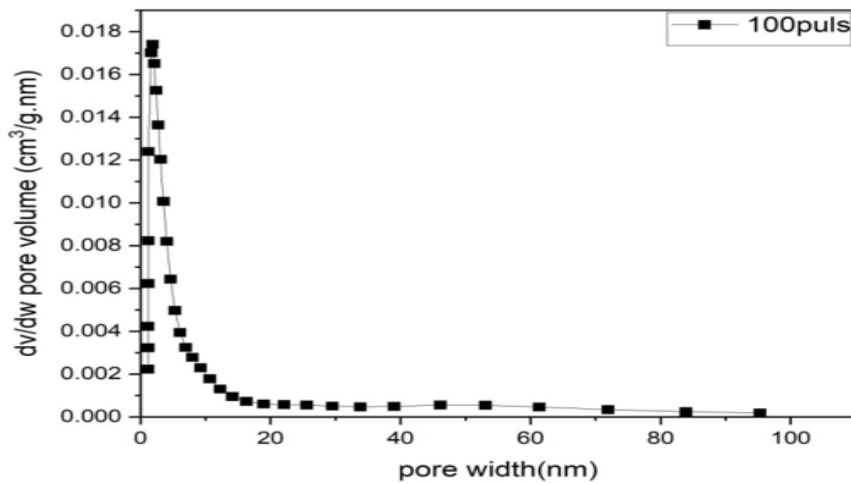


Fig. (14) Pore size distribution of TiO<sub>2</sub> by laser ablation method at 100puls.

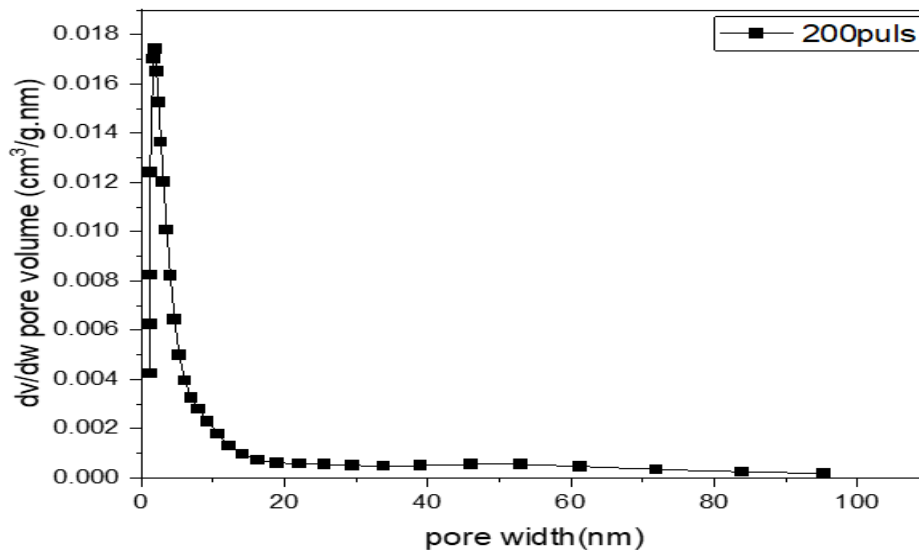


Fig. (15) Pore size distribution of TiO<sub>2</sub> by laser ablation method at 200 pulse

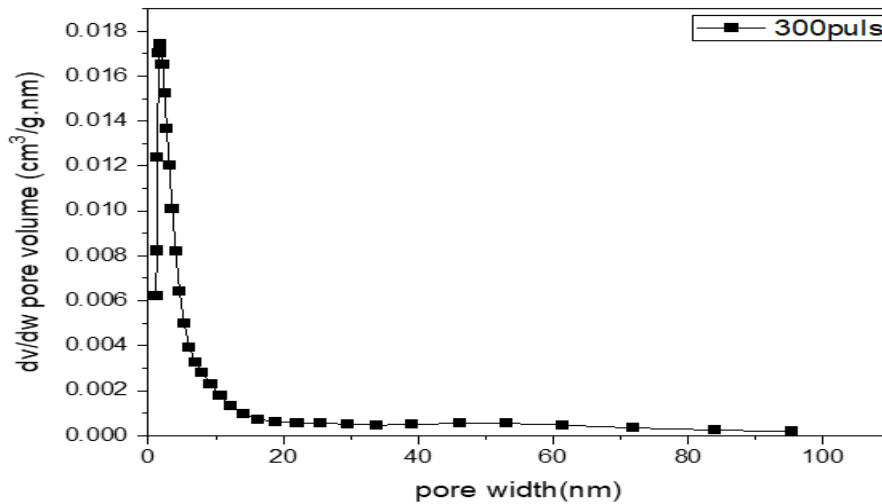


Fig. (16): Pore size distribution of TiO<sub>2</sub> by laser ablation method at 300 pulse.

Table (5): Surface area, average pore diameter and volume of TiO<sub>2</sub> nanoparticles samples prepared at (100puls,200puls,300puls) by laser ablation method.

Laser pulse	Surface area (m <sup>2</sup> /g <sup>-1</sup> )	Average pore diameter (nm)	Total pore volume (m <sup>3</sup> /g)
100pulse	82.44	3.52	0.044
200pulse	86.43	3.57	0.047
300pulse	98.67	5.28	0.048

3.3 (Energy dispersive x-ray)EDX

Figure(17,18,19)represents the EDX spectra of TiO<sub>2</sub> nanoparticles prepared at 40%, 60%, and 100% by the microwave method. The EDX

analyses affirmed the atomic composition of the prepared samples. The results show that the spectra consisted of titanium (Ti) and oxygen (O) peaks with high intensity,

indicating the successful synthesis of pure TiO<sub>2</sub> nanoparticles. The other weak peaks were attributed to impurities during the sample preparation for EDX analysis, such as silicon (Si).

Through the EDX results, we notice the appearance of Si peaks, and this is due to the Si used in the working

method. From EDX analysis, the elemental percentages of Ti in microwave method were found to be (31.49%, 26.92%, and 23.22 %), while elemental percentages of oxygen (O) were found to be (68.51%, 73.08%, and 76.78 %) in the prepared samples (40%,60%,100%)respectively.

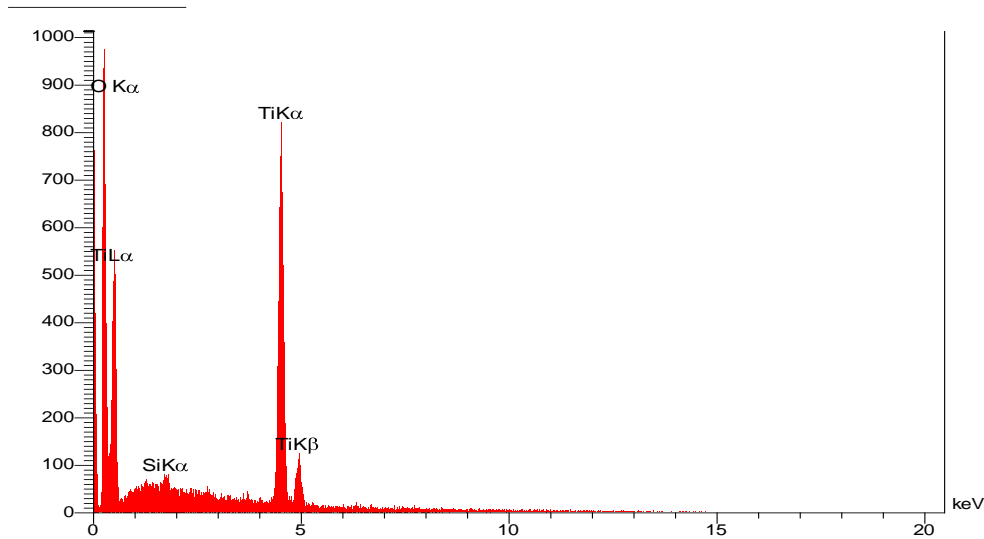


**Fig. (17):** EDX spectrum of TiO<sub>2</sub> Nanoparticles at 40%.

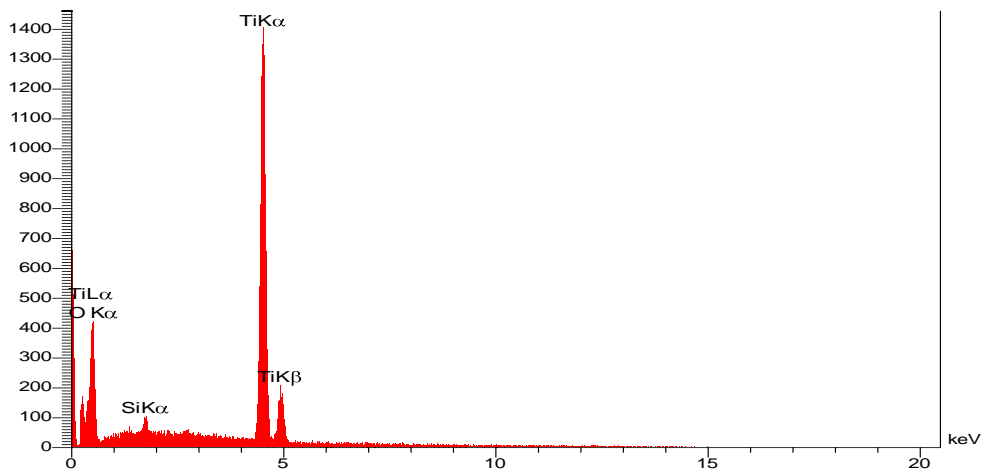


**Fig. (18):** EDX spectrum of TiO<sub>2</sub> Nanoparticles at 60%.

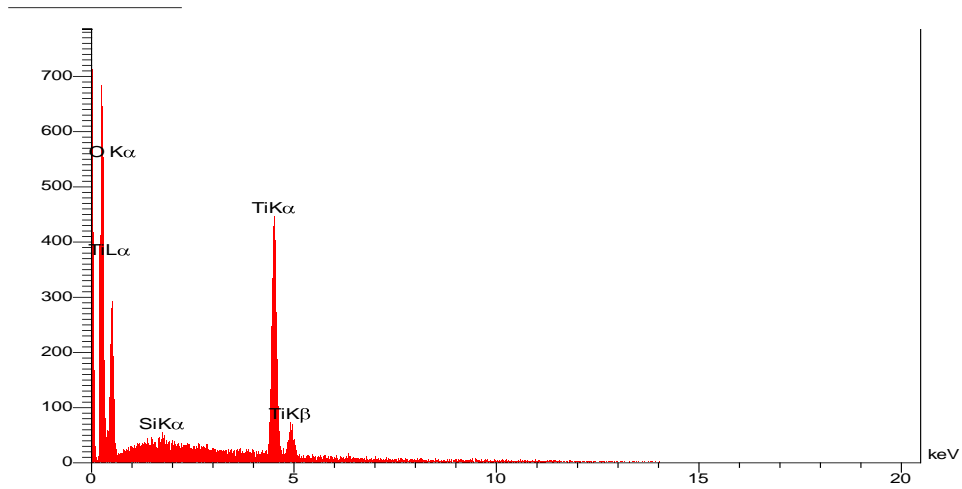


**Fig. (19):** EDX spectrum of TiO<sub>2</sub> Nanoparticles at 100%.

The EDX spectra of TiO<sub>2</sub> nanoparticles synthesized via laser ablation at 100 puls, 200 puls, and 300 puls are illustrated in Figures 11, 12, and 13. The EDX analyses confirmed that the produced samples had the specified atomic composition. The findings demonstrate that the spectra comprised intense peaks for titanium (Ti) and oxygen (O), which provide confirmation that the synthesis of pure TiO<sub>2</sub> nanoparticles was effective.

Through the EDX results, we notice the appearance of Si peaks, and this is due to the Si used in the working method. From EDX analysis, the elemental percentages of Ti in laser ablation were found to be (28.22 %, 24,03% and 19.22 %) while elemental percentages of oxygen (O) were found to be (71.78 %, 75.97%, and 80,78 %) in the prepared samples (40%, 60%, 100%) respectively.

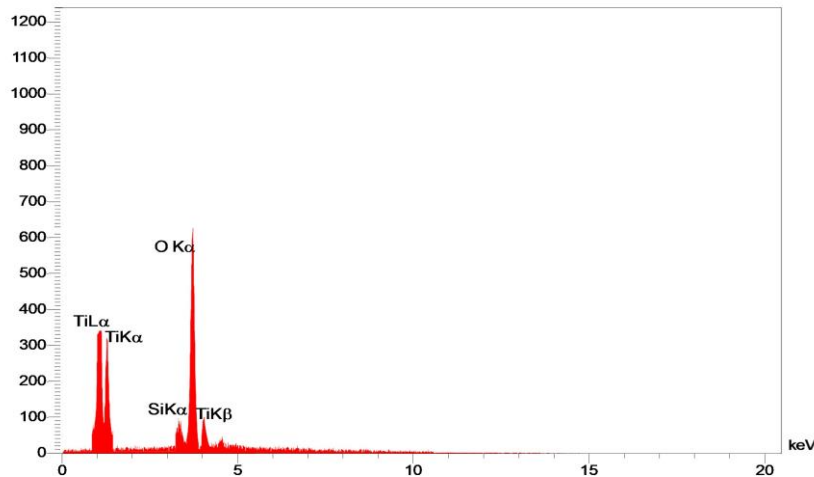


**Fig. (20)** EDX spectrum of TiO<sub>2</sub> nanoparticles by laser ablation at 100 pulse.

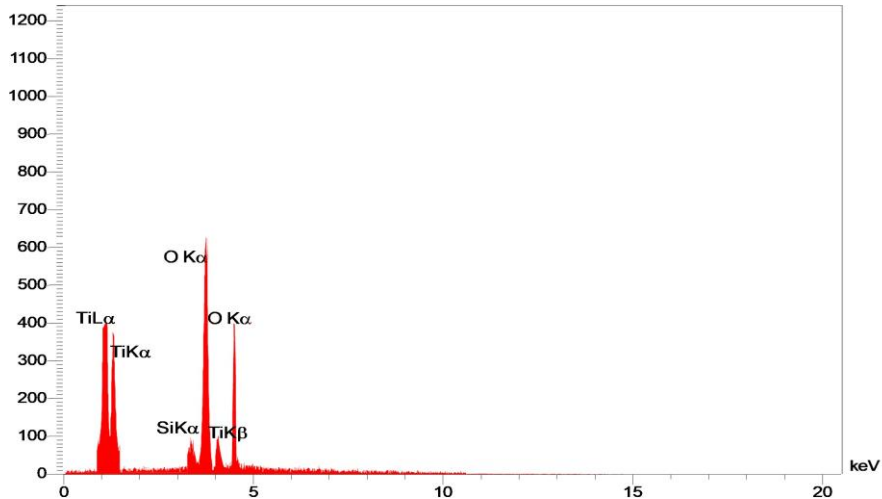


Fig. (21) EDX spectrum of TiO<sub>2</sub> nanoparticles by laser ablation at 200 pulse.

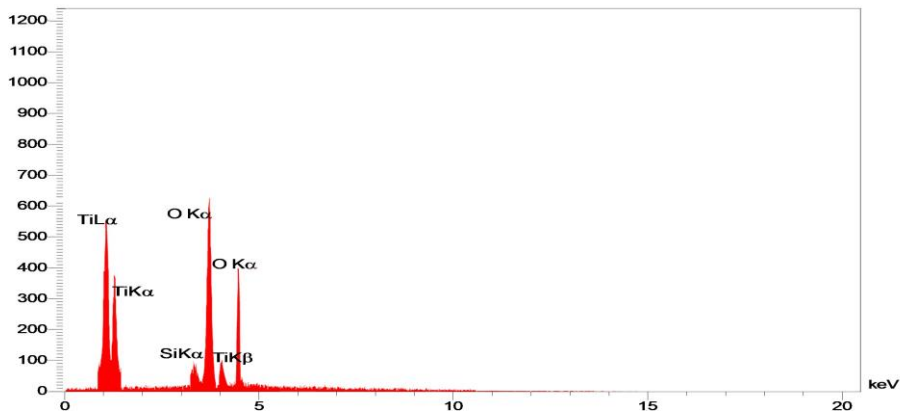


Fig. (22) EDX spectrum of TiO<sub>2</sub> nanoparticles by laser ablation at 300 pulse.

#### 4. Conclusion

The findings of this work indicate that the use of microwave technology with pulsed laser ablation offers a succinct, expeditious, and user-friendly approach to generate titanium dioxide nanoparticles. in microwave method. The XRD analysis deduced that the TiO<sub>2</sub> nanoparticles synthesized in this work exist in the anatase TiO<sub>2</sub> phase. The diffraction peaks of the prepared samples detect a sharp domain (101) peak at about  $2\theta=25.28^\circ$ . The X-ray patterns also showed that there

are no peaks of other materials, indicating the samples were prepared with a high degree of purity, in laser ablation the XRD analysis deduced that the TiO<sub>2</sub> nanoparticles synthesized in this work exist in the brookite TiO<sub>2</sub> phase. The BET analysis in microwave technology with pulsed laser ablation revealed that the samples showed a type IV isotherm. It can be noticed that the microwave technology samples have a higher surface area and a higher pore size. The EDX results revealed that the spectra consisted of Titanium (Ti) and Oxygen (O) peaks with

high intensity indicating the successful

synthesis of pure TiO<sub>2</sub> nanoparticles.

## References:

- [1]Pang CL, Lindsay R, Thornton G. Chemical reactions on rutile TiO<sub>2</sub> (110). *Chemical Society Reviews*. 2008;37(10):2328-2353.
- [2]Kumar A. Different methods used for the synthesis of TiO<sub>2</sub> based nanomaterials: A review. *Am J Nano Res Appl*. 2018;38(1):2243-2531.
- [3] Ding B, Kim CK, Kim HY, Seo MK, Park SJ. Titanium dioxide nan fibers prepared by using electro spinning method. *Fibers and Polymers*. 2004;5(2):105-109.
- [4] Cadre JG, Molina-Prado's S, Mingles-Vega G, Estrada AC, Trinidad T, Oliveira C, et al. Multifunctional silver-coated transparent TiO<sub>2</sub> thin films for photocatalytic and antimicrobial applications. *Appl Surf Sci*. 2023;61(7):156-519
- [5] Barnard AS, Zapol P, Curtiss LA. Modeling the morphology and phase stability of TiO<sub>2</sub> nanocrystals in water. *J Chem Theory Compute*. 2005;1(1):107-16.
- [6] Mute DK, Deena BF., The effect of tetra isopropyl orthotitanate (TIP) concentration on structural, and luminescence properties of titanium dioxide nanoparticles prepared by sol-gel method. *Mater Sci Semi Cond Process*. 2020;10(6):104-783.
- [7]Reda S. Jalawkhan, Firas K. Mohamed Alosfur,Ahmed M. Abdul-Lettif. "Characterization of pure anatase TiO<sub>2</sub> nano rods synthesized by microwave method", AIP Publishing, 2022.
- [8] Liu C. A study of particle generation during laser ablation with applications. Doctoral Thesis, University of California, Berkeley; 2005.
- [9] Mufeed Abbas G. Fabrication and Characterization of TiO<sub>2</sub> Dye-sensitized Solar Cells. 2020.
- [10] Nickname, Vorname; Zu Göttingen, Akademie der Wissenschaften. Wahrheit. Wahrheit, 2023.
- [11] Cao K. Sustainable porous hollow carbon spheres with high specific surface area derived from Kraft lignin. *Advanced Powder Technology*. 2021;7(3):20-64.
- [12]Reda S. Jalawkhan, Aseel Adnan Ouda,Ahmed M. Abdul-lettif, Firas K. MohamadAlosfur. "Effect of solvents on the morphologyof TiO<sub>2</sub> nanoparticles prepared by microwavemethod", IOP Conference Series: Materials Science and Engineering, 2020.